Heliyon 9 (2023) e16491

Contents lists available at ScienceDirect

Heliyon

journal homepage: www.cell.com/heliyon

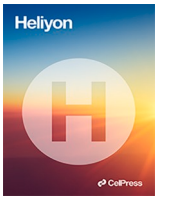

Research article

Characterization of new natural cellulosic fiber from *Calamus tenuis* (Jati Bet) cane as a potential reinforcement for polymer composites

Arup Kar [a,*], Dip Saikia [b]

[a] *Department of Physics, Dibrugarh University, Assam, India*
[b] *Department of Physics, Digboi College, Digboi, Assam, India*

ARTICLE INFO

Keywords:
Calamus tenuis cane fibers
Chemical analysis
Crystalline properties
Thermal analysis
Mechanical properties
Morphological properties

ABSTRACT

This study investigates the physical, structural, chemical, thermal, mechanical, and morphological properties of the fibers of *Calamus tenuis* canes and compares the findings with various lignocellulosic fibers to find the place of these fibers as reinforcements for polymer composites. Chemical analysis confirms the presence of 37.43 ± 1.40% cellulose, 31.06 ± 1.03% hemicellulose, and 28.42 ± 0.81% lignin in *Calamus tenuis* cane fibers, moreover, the presence of these constituents is also confirmed by Fourier Transformed Infrared Spectroscopic (FTIR) analysis. The X-Ray diffraction (XRD) analysis determines the crystallinity index of 37.38 ± 0.27% and the crystallite size of 0.87 ± 0.03 nm of the samples. The thermogravimetric analysis ensures that the *Calamus tenuis* cane fibers are thermally stable up to 210 ± 5 °C. The Weibull distribution analysis is employed to estimate the tensile properties of *Calamus tenuis* canes, which reveal a tensile strength of 37.5 ± 2 MPa, Young's modulus of 1.05 ± 0.08 GPa, and an elongation at break of 18.94 ± 4.26%. The roughness of the fibers' outer surface is confirmed by SEM micrographs and AFM analysis, suggesting that it could enhance the adhesion between fibers and matrix during the fabrication of composites.

1. Introduction

A growing awareness of environmental issues, new government regulations aimed at protecting the environment, and consumer demands have prompted the scientific community and manufacturing industry to come up with new reinforcing materials that could serve as alternatives to commonly used non-renewable reinforcing materials [1,2]. Over the past few decades, the composite industries have shown significant interest in natural fibers, particularly those derived from plants, owing to their renewable source, widespread availability, lightweight, low density, relatively good mechanical strength, and other desirable properties. Natural fibers have found use as reinforcements in polymer composites for a range of applications, including building materials, swimming pool panels, sports equipment, aircraft parts, backrests, and automotive components, among others [3–5].

Understanding the properties of fibers is crucial before fabricating composites, as the quality of composites relies on two factors (i) the characteristics of the fibers and matrix, and (ii) the strength of the interfacial bondings between them. Moreover, the physical properties of the fibers should be in line with the requirements of the intended application. Literature indicates that cellulose, lignin,

* Corresponding author.
E-mail address: arupkar472@gmail.com (A. Kar).

https://doi.org/10.1016/j.heliyon.2023.e16491
Received 6 March 2023; Received in revised form 4 May 2023; Accepted 18 May 2023
Available online 23 May 2023

hemicellulose, pectin, wax, etc. are the main constituents of the plant fibers, and chemical treatments may be necessary to modify the fibers' surface to use them as reinforcements for polymer composites [6,7].

Several natural fibers including *Calotropis gigantea* [1], *Ferula communis* [2], *Chloris barbata* [3], *Tridax procumbens* [4], *Prosopis juliflora* bark [8], *Furcraea foetida* [9], *Putranjiva roxburghii* W. Seed Shell [10], etc. have been extracted and characterized by many researchers and many of these natural fibers have also been utilized as reinforcement during composite fabrication.

Calamus tenuis (Jati Bet) is a common cane of North East India referred to as Assam cane in commerce [11]. These canes have been used for manufacturing lightweight furniture, decorative items, etc. Handicraft industries consider them to be exceptional and versatile raw materials due to their lightness, durability, and flexibility. But the fibers of *Calamus tenuis* (Jati Bet) canes have not been studied yet to find their place as reinforcements for polymer composites. In this work, attempts have been made to investigate the physicochemical, thermal, and mechanical characterization of raw *Calamus tenuis* (Jati Bet) cane fibers, and their evaluated characteristic parameters have been compared with that of various natural fibers determined by many researchers. In this investigation, the characteristic features of raw *Calamus tenuis* cane fibers have been analyzed by chemical composition analysis, Fourier Transformed Infrared Spectroscopy (FTIR), X-Ray Diffraction (XRD), Thermogravimetric Analysis (TGA), Test for mechanical properties, Scanning Electron Microscopy (SEM), and Atomic Force Microscopy (AFM).

2. Materials and methods

2.1. Extraction of Calamus tenuis cane fibers

Raw materials of *Calamus tenuis* (Jati Bet) were obtained from the Naharkatia region (27.2870° N, 95.2476° E) of Dibrugarh District, Assam, India. The canes were submerged in water for a duration of 14 days after extraction, to facilitate microbial degradation [8] and also to soften the outermost layers of *Calamus tenuis* canes. The outermost layers of the canes were separated manually. After separation, the canes underwent a washing process in distilled water to eliminate undesired impurities such as sand, dust, and other particles adhering to the surface. Following this, they were sun-dried for a duration of 8 days. The techniques outlined elsewhere were employed to prepare the different samples of *Calamus tenuis* cane fibers required for the current study [12]. Fig. 1(a) shows the *Calamus tenuis* cane tree, and Fig. 1(b) shows the extracted canes from *Calamus tenuis* tree.

2.2. Characterization of Calamus tenuis cane fibers

2.2.1. Measurement of bulk density, true density, porosity, and diameter

The bulk density (ρ_b) of cylindrical *Calamus tenuis* canes was determined in accordance with KSF 2198 [13,14] by using

$$\rho_b = \frac{W}{V} \tag{1}$$

in Eq. (1), W represents the weight of the sample, while V denotes its volume.

The true density of the samples was measured by a gas pycnometer (Model: PYC-100A, Porous Materials Inc, Make: Ithaca, New York, USA). For the measurement of true density, the true volume of the solid sample is calculated from the pressure drop when air at a certain pressure is allowed to expand into the chamber containing the sample. The true density (ρ_t) is measured by using the following formula:

$$\rho_t = \frac{W}{V_t} \tag{2}$$

In Eq. (2), W, and V_t represents the weight, and true volume of the sample respectively.

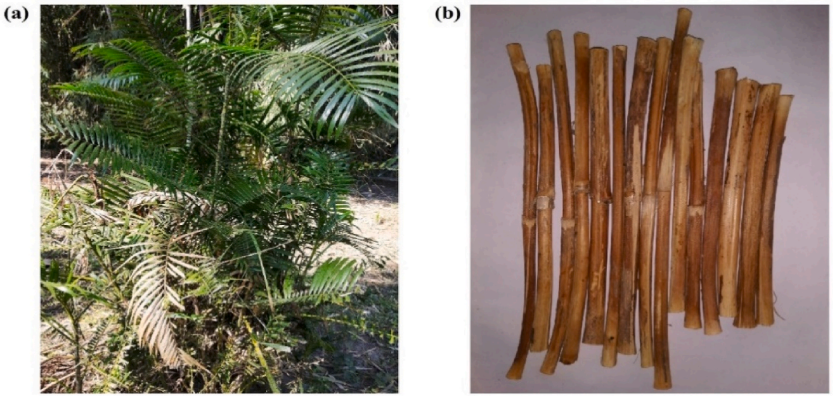

Fig. 1. (a) *Calamus tenuis* tree, (b) Canes extracted from *Calamus tenuis* tree.

Porosity measures the percentage of void spaces in a material. Porosity (ε) of the sample is estimated by using the following formula [15]:

$$\varepsilon = \left(1 - \frac{\rho_b}{\rho_t}\right) \times 100\% \tag{3}$$

In Eq. (3), ρ_b represents the bulk density, and ρ_t represents the true density of the sample.

The diameter of the 20 samples of *Calamus tenuis* canes at 3 different places was measured using a screw gauge and the average value was presented.

2.2.2. Chemical analysis

The chemical composition of the *Calamus tenuis* cane fibers was estimated by using chemical analysis. For this purpose, standard methods were employed. The percentage contents of cellulose in the *Calamus tenuis* fibers were estimated by Undegraff Method [16]. The natural detergent fiber (NDF) method was employed to estimate the hemicellulose contents [17]. Lignin contents were estimated by using TAPPI T 222 om-02 method. ASTM D4442-07 and TAPPI T 211 om-02 were used for moisture and ash contents estimation respectively. Acid hydrolysis was used to extract the pectin and also to estimate its content in *Calamus tenuis* cane fibers. Three replicates were performed for all the chemical analyses and the average result was presented.

2.2.3. Fourier Transformed Infrared (FTIR) analysis

Fourier Transformed Infrared (FTIR) Spectroscopy technique identifies the functional groups present in the *Calamus tenuis* cane fibers. For this purpose, 1 mg powder of *Calamus tenuis* cane fibers was mixed with KBr to form pellets. The pellets underwent testing using a Nicolet Impact 410 FTIR Spectrometer (USA), with 1 cm^{-1} resolution, within the wave number range of 400 cm^{-1} to 4000 cm^{-1}.

2.2.4. X-Ray Diffraction (XRD) analysis

X-Ray Diffraction (XRD) Analysis of *Calamus tenuis* cane fibers was carried out by PANalytical Empyrean Powder XRD at 25 °C to know the crystalline properties of the samples. The spectrum was recorded between 5° and 80° (2θ angle) with 0.0260° step size. The generator was set at 45 kV and 40 mA. Segal's Equation determined the crystallinity index (CI) of *Calamus tenuis* cane fibers [18].

$$\mathrm{CI} = \left(1 - \frac{I_{am}}{I_{002}}\right) \times 100\% \tag{4}$$

In Eq. (4), I_{002} represents the intensity peak at 22° corresponding to the crystallographic plane (002) (crystalline region), I_{am} represents the intensity peak at around 18° lying between the planes (002) and (101) (amorphous region). Scherrer's Equation was employed to compute the Crystallite Size (CS) of *Calamus tenuis* cane fibers [2].

$$\mathrm{CS} = \frac{K\lambda}{\beta\, COS\, \theta} \tag{5}$$

In Eq. (5), λ denotes the wavelength of CuK_α radiation, Scherrer's constant is K = 0.89, β represents the peak's FWHM, and θ represents Bragg's angle.

2.2.5. Thermogravimetric Analysis (TGA)

The degradation characteristics of *Calamus tenuis* cane fibers were measured using a METTLER TOLEDO Thermogravimetric Analyser. To conduct the analysis, approximately 5 mg of *Calamus tenuis* cane fiber powder was heated at a rate of 10 °C per minute in an alumina crucible, over a temperature range of 25 °C–700 °C. Throughout the analysis, a nitrogen atmosphere was maintained with a gas flow rate of 20 mL per minute. The kinetic activation energy (E_a) was evaluated from Coats and Redfern equation [19].

$$\ln[-\ln(1-x)] = \ln\frac{ART^2}{\beta E_a} - \frac{E_a}{RT} \tag{6}$$

In Eq. 6, A is the pre-exponential factor, β denotes the rate of heating (10 °C per minute), R is the universal gas constant (8.32 kJ $mol^{-1}K^{-1}$), T represents the absolute temperature in Kelvin (K), and $x = \frac{w_0 - w_t}{w_0 - w_f}$, where w_0, and w_t represents the initial weight, and the weight of the sample at a particular time. w_f be the final weight of the sample. Kinetic activation energy is calculated by plotting the graph between $\ln[-\ln(1-x)]$ vs 1000/T.

2.2.6. Study of mechanical properties

2.2.6.1. Tensile test. The INSTRON 8801 Universal Testing Machine (UTM) equipped with a 100 kN load cell was employed to measure the tensile properties of *Calamus tenuis* canes at a temperature of 24 °C. A total of twenty samples were tested with a gauge length of 50 mm and a cross head speed of 1 mm per minute. The laboratory was maintained at a relative humidity of 55% throughout the testing process. The tensile properties data were analyzed using the Weibull distribution analysis with the aid of Minitab 17

software. The formula used to calculate the microfibril angle (α) in degree of *Calamus tenuis* cane fibers is given below [20].

$$\varepsilon = ln\left(1 + \frac{\Delta L}{L_0}\right) = -\ln(cos\ \alpha) \tag{7}$$

In Eq. (7), ε is the strain, L_0, and ΔL represents the gauge length and elongation at break in mm respectively.

2.2.6.2. Flexural test. The INSTRON 8801 UTM equipped with a 100 kN load cell was used at 24 °C with Relative humidity of 55% for conducting a three-point bending test in order to determine the flexural strength and flexural modulus of *Calamus tenuis* canes. The tests were performed at a cross head speed of 2.5 mm per minute, with a span length of 50 mm.

2.2.7. Scanning Electron Microscope (SEM) analysis

The JSM 6390LV SEM was employed to examine the surface morphologies of *Calamus tenuis* canes. The SEM was operated at 20 kV, using magnifications of 50×, 100×, and 200×. To prevent charging of the non-conductive samples, they were coated with gold prior to analysis.

2.2.8. Atomic Force Microscope (AFM) analysis

The surface roughness of *Calamus tenuis* cane fibers was studied using high-resolution 2D and 3D imaging techniques provided by Atomic Force Microscopy (AFM). In this study, the Atomic Force Microscope, Model: NTEGRA Prima, manufactured by NT-MDT Technology was used. A Standard Si cantilever with a scanning rate of frequency 1 Hz was used for scanning the samples. Various surface roughness parameters, including root mean square roughness (S_q or S_{rms}), mean roughness (S_a), surface skewness (S_{sk}), ten points average absolute height roughness (S_z), maximum peak-to-valley height (S_t), and kurtosis (S_{ku}) were estimated.

3. Results and discussions

3.1. Measurement of bulk density, true density, porosity, and diameter

The bulk density of *Calamus tenuis* canes is evaluated by using Eq. (1). and it is estimated as 526 ± 16 kg m^{-3} whereas the true density is 720 ± 16 kg m^{-3} computed from Eq. (2). The comparison of the density of *Calamus tenuis* canes with that of various natural fibers determined by some researchers is shown in Table 1, which depicts that this value is less as compared to other natural fibers. The low value of density reveals that *Calamus tenuis* canes can be used in lightweight polymer composite applications [8,9,21]. The porosity of the sample is measured by using Eq. (3). and this value is found to be 27.77%, which confirms the porous structure of the *Calamus tenuis* canes, and is also in good agreement with the SEM results. Measuring the diameter of plant fibers is a challenging task due to their irregular shape along their length. However, for the measurement of tensile property, it is assumed to be circular. The average diameter of the *Calamus tenuis* canes is found to be 8.31 ± 0.48 mm.

Table 1
Comparison of density of *Calamus tenuis* canes with various natural fibers.

Name of Fibers	Density (kg m^{-3})
***Calamus tenuis* (Bulk Density)**	**526 ± 16**
***Calamus tenuis* (True Density)**	**720 ± 16**
Calotropis gigantea Bast [1]	1324
Ferula communis [2]	1240
Chloris barbata [3]	634
Tridax procumbens [4]	1160 ± 120
Areca Palm Leaf Stalk [5]	1090 ± 24
Prosopis juliflora bark [8]	580
Furcraea foetida [9]	778
Cyrtostachys renda [21]	1020
Arundo Donax L. [22]	1168
Musa textilis [23]	1500
Stipa tenacissima [24]	890–1400
Acacia leucophloea [25]	1382
Calamus manan (Bulk Density) [26]	450
Cissus quadrangularis stem [27]	1220
Coccinia grandis L. [28]	1243 ± 22.6
Corn Husk [29]	340
Corypha taliera fruit [30]	860
Juncus effusus L. [31]	1139
Palm Tree Leaf Stalk [32]	850
Wikstroemia Spp. [33]	1023
Raffia textilis [34]	750
Saccharum spontaneum [35]	1188 ± 8
Furcraea foetida leaves [36]	1165.78 ± 52.20

3.2. Chemical analysis

The chemical composition of *Calamus tenuis* cane fibers and various natural fibers are listed in Table 2. It shows that cellulose content in *Calamus tenuis* cane fibers is 37.43 ± 1.40%. Cellulose is one of the important constituents that provide good mechanical strength to cane fibers [24,33]. Apart from providing mechanical strength to cane fibers, cellulose also contributes toughness, and structural steadiness to the samples [22,30]. The hemicellulose content of *Calamus tenuis* cane fibers is found to be 31.06 ± 1.03%, which is comparable with many other lignocellulosic fibers. But the hemicellulose content can disintegrate the fibers, resulting in lower strength of lignocellulosic fibers [8]. This defect can be modified by treating the samples with alkali of suitable proportions [37]. The higher percentage of lignin (28.42 ± 0.81%) in *Calamus tenuis* cane fibers contributes to resistance against microbial attack [22] and gives superior structural rigidity to the fibers [8]. The pectin content in *Calamus tenuis* cane fibers is very less and is estimated to be 0.51 ± 0.12%. The moisture content of *Calamus tenuis* cane fibers is estimated to be 10.57 ± 1.53%. The moisture content confirms the presence of hemicellulose in samples [38]. The ash content of the sample is found to be 4.11 ± 0.62%.

3.3. Fourier Transformed Infrared (FTIR) analysis

Fig. 2 shows FTIR spectra of *Calamus tenuis* cane fibers. A wide peak was observed at 3419.69 cm^{-1}, which is attributed due to the stretching vibration of hydrogen bonds and –OH present in hydroxyl groups [9,21,22,28]. Two less intense peaks at 2928.04 cm^{-1} and 2848.42 cm^{-1} are observed due to the C–H stretching vibrations, which confirm the presence of cellulose and hemicellulose [5,22,41]. The peak observed at 1738.71 cm^{-1} is associated with the vibrations C═O group of hemicellulose or to the ester bonds within the carboxylic groups in lignin [20,21,32]. A peak at 1634.37 cm^{-1} is connected with the C═O (Carbonyl Groups) linkage of hemicellulose and lignin [2,5]. The peak observed at around 1507.25 cm^{-1} is associated with the stretching vibration of C═C of the phenyl propane group in aromatic lignin [41]. The absorption peak observed at 1425.92 cm^{-1} is due to the presence of symmetric bending of CH_2 in cellulose [20,22]. The peak at 1375.10 cm^{-1} belongs to the C–H group of cellulose [20]. The vibration peak observed at 1247.05 cm^{-1} indicates the stretching vibration of C–O of acetyl groups in lignin [46] or C═O stretching of hemicellulose [28,34,45]. The characteristics peak observed at 1072.22 cm^{-1} manifests the existence of C–O groups of cellulose [5,41]. A peak at around 898.07 cm^{-1} may be due to the β-glycosidic bonds of monosaccharides [20,45]. A peak observed at 606.84 cm^{-1} may be due to the bending of C–OH [20,22].

3.4. X-Ray Diffraction (XRD) analysis

The XRD spectrum of *Calamus tenuis* cane fibers is presented in Fig. 3. The diffractogram contains mainly three diffraction peaks. The most prominent and intense peak, occurring at approximately $2\theta = 22^{\circ}$, corresponds to the Miller indices of the (200) plane, and is attributed to the presence of cellulose I [8,27,29,35]. Two additional diffraction peaks of lower intensity can be seen at $2\theta = 16^{\circ}$ and 34.5°, which correspond to the crystal planes (101) and (004), respectively [2,30]. The crystallinity index is estimated using Eq. (4).

Table 2
Comparison of Chemical composition of *Calamus tenuis* cane fibers with various natural fibers.

Name of fibers	Cellulose (%)	Hemicellulose (%)	Lignin (%)	Ash (%)	Moisture (%)
Calamus tenuis	**37.43 ± 1.40**	**31.06 ± 1.03**	**28.42 ± 0.81**	**4.11 ± 0.62**	**10.57 ± 1.53**
Calotropis gigantea Bast [1]	63.56	19.29	10.38	5.78	–
Ferula communis [2]	53.3	8.5	1.4	7.0	24.8
Chloris barbata [3]	65.3	10.23	9.32	2.52	7.29
Tridax procumbens [4]	32	6.8	3	–	11.2
Areca Palm Leaf Stalk [5]	57.49 ± 0.66	18.34 ± 0.24	7.26 ± 0.12	1.49 ± 0.01	9.35 ± 0.15
Prosopis juliflora bark [8]	61.65	16.14	17.11	5.2	9.48
Furcraea foetida [9]	68.35	11.46	12.32	6.53	5.43
Calamus manan [20]	42	20	27	–	–
Cyrtostachys renda [21]	45.15	22.88	18.77	–	–
Arundo donax L. [22]	43.2	20.5	17.2	1.9	–
Acacia leucophloea [25]	68.09	13.60	17.73	–	–
Cissus quadrangularis stem [27]	82.73	7.96	11.27	–	6.6
Coccinia grandis L. [28]	62.35	13.42	15.61	4.388	5.6
Corn Husk [29]	46.15	33.79	13.92	–	11.961
Corypha taliera fruit [30]	55.1	21.78	17.6	–	7.1
Palm Tree Leaf Stalk [32]	44.10	13.02	4.52	–	–
Wikstroemia Spp. [33]	79.05	13.6	10.13	60.93	50.21
Saccharum spontaneum [35]	43.2 ± 1.2	26.2 ± 0.3	22.4 ± 0.3	–	6.80 ± 0.20
Agave americana L. [38]	71.65 ± 1.20	22.4 ± 0.9	6.09 ± 0.3	–	5.26 ± 0.06
Musa textilis [39]	66.43	30.7	13.6	–	0.7
Stipa tenacissima [40]	46 ± 3	24 ± 2	20 ± 2	7.2 ± 1	–
Juncus effuses [41]	56.9	28.2	9.9	–	–
Lufa Sponge [42]	57.51 ± 0.2	29.47 ± 0.25	17.37 ± 0.23	–	8.83 ± 0.30
Pennisetum purpureum stem [43,44]	45.66	33.67	20.60	–	13.9 ± 1.1
Saharan Aloevera Cactus Leaves [45]	60.2	14.2	13.7	–	7.6

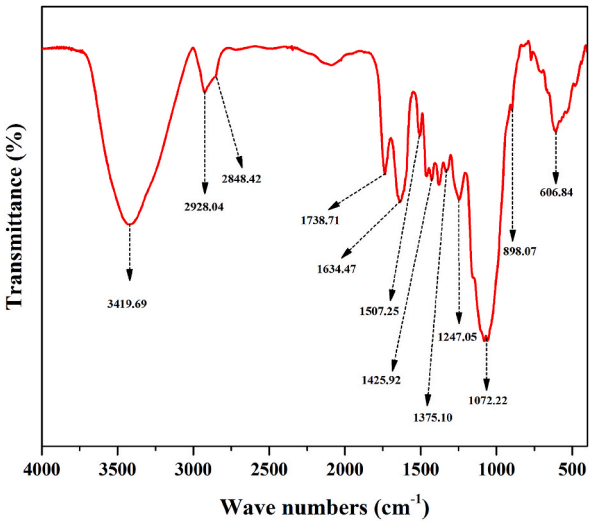

Fig. 2. FTIR Spectra of *Calamus tenuis* cane fibers.

and for *Calamus tenuis* cane fibers this value is calculated to be 37.38 ± 0.27%, which is higher than many natural fibers like *Tridax procumbens* [4], *Juncus effusus* L. [30], and Lufa Sponge [42]. The Crystallite size of *Calamus tenuis* cane fibers is estimated using Eq. (5). as 0.87 ± 0.03 nm, which is lower than many natural fibers like *Cissus quadrangularis* stem [27], *Corypha taliera* fruit [30], *Calamus manan* [20], Sisal [47], Areca Palm Leaf Stalk [48], etc. The crystallite size reduces the chemical reactivity as well as the hydrophilicity of the fibers during the composite fabrication. The chemical modification of these raw fibers of *Calamus tenuis* canes can improve the degree of the structural arrangement of the fibers [30]. The comparison of crystalline properties of *Calamus tenuis* cane fibers with that of various natural fibers determined by some researchers is shown in Table 3.

3.5. Thermogravimetric Analysis (TGA)

Fig. 4(a) shows the TGA and DTG graphs of *Calamus tenuis* cane fibers, which exhibit three stages of thermal decomposition. A minor weight loss of 13.03% is observed between 25 °C and 110 °C in the first stage is attributed to the sample's hydrophilic properties [21,22,27,41,51]. *Calamus tenuis* cane fibers show thermal stability up to 210 ± 5 °C. In the 2nd stage, a weight loss of 53.71% is recorded in the temperature range from 210 °C to 351 °C, where two peaks with peak temperatures of 293 ± 3 °C and 315 ± 1 °C are observed. The initial peak, seen at 293 ± 3 °C and accompanied by a weight loss of 39.39%, suggests the decomposition of hemicellulose, pectin, and glycosidic bonds within the sample's cellulose [22,27,34,43]. The second peak observed at 315 ± 1 °C accompanied by a weight loss of 54.52% is attributed to α-cellulose decomposition [22,27,34,51]. A single peak at 453 ± 2 °C is observed in the temperature range from 351 °C to 700 °C which is due to the degradation of lignin [34,51]. Similar results of three stages of thermal decomposition are also observed in various natural fibers investigated by some researchers which are listed in

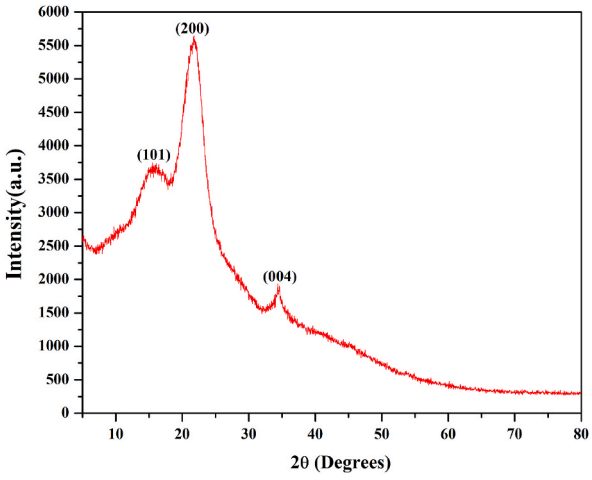

Fig. 3. XRD diffractogram of *Calamus tenuis* cane fibers.

Table 3
Comparison of Crystalline properties of *Calamus tenuis* cane fibers with various natural fibers.

Name of fibers	Crystallinity Index (%)	Crystallite Size (nm)
Calamus tenuis	**37.38 ± 0.27**	**0.87 ± 0.03**
Calotropis gigantea Bast [1]	80.9	–
Ferula communis [2]	48	1.6
Chloris barbata [3]	50.29	–
Tridax procumbens [4]	34.46	25.04
Prosopis juliflora bark [8]	46	15
Furcraea foetida [9]	52.6	28.36
Calamus manan [20]	48.28	1.91
Cyrtostachys renda [21]	50	–
Acacia leucophloea [25]	51	15
Cissus quadrangularis stem [27]	47.15	3.91
Coccinia grandis L. [28]	52.17	13.38
Corn Husk [29]	43.7	2.25
Corypha taliera fruit [30]	62.5	1.45
Juncus effusus L. [31]	33.40	3.6
Palm Tree Leaf Stalk [32]	46.37	–
Raffia textilis [34]	51	9.6
Saccharum spontaneum [35]	53	–
Furcraea foetida leaves [36]	62.05	2.44
Stipa tenacissima stem [37]	59.5	–
Agave americana L. [38]	53.2	–
Lufa Sponge [42]	24.4 ± 1.4	–
Saharan Aloevera Cactus Leaves [45]	52.6	5.6
Sisal [47]	51.23	3.156
Areca Palm Leaf Stalk [48]	44	31.6
Arundo donax L. [49]	53.8	–
Ceiba aesculifolia Seed Pods [50]	63	–
Date Palm [51]	57.14	–

Table 4. Fig. 4(b) shows the graph between $\ln[-\ln(1-x)]$ vs 1000/T and the activation energy (E_a) of the samples is evaluated slope the graph. The activation energy for the thermal stability of the samples is found to be 57.01 kJ/mol which is nearly equal to Saharan Aloevera Cactus Leaves (60.2 kJ/mol) [45], but lower than many other cellulosic fibers such as *Furcraea foetida* (65.64 kJ/mol) [9], *Cissus quadrangularis* stem (65.23 kJ/mol) [27], *Calamus manan* (81.68 kJ/mol) [20] The above results confirmed that *Calamus tenuis* cane fiber can be used as reinforcement element for bio-composites which can operate up to 315 ± 1°.

3.6. Study of mechanical properties

3.6.1. Tensile test

Fig. 5(a) represents the Tensile Stress-Tensile Strain curve of *Calamus tenuis* canes. It exhibits brittle behavior of the samples when failures occur. There are three stages of deformation in the Stress-Strain curve (Fig. 5(a)). At first, *Calamus tenuis* canes exhibit linear deformation up to a strain value of 0.44% which could be attributed to the total loading of the canes by cell wall deformation [22,45]. Secondly, the stress-strain curve shows non-linear behavior from 0.44% to 6.9%, which may be due to the deformation of elasto-visco-plastic of the samples [22,45]. Finally, linear deformation is observed from around 6.9% strain until failure of the canes, which attributes to the elasticity of microfibrils alignment towards the applied tensile strain [22,45]. Fig. 6(a-c) shows the plot of the Weibull distribution of tensile strength, young's modulus, and elongation at break, where, the values are positioned on the line and fit the Weibull distribution perfectly. From the Weibull distribution, it is found that the tensile strength of *Calamus tenuis* canes is 37.5 ± 2 MPa, which is close to the value of plant fibers such as bulk *Calamus manan* [26], *Corypha taliera* fruit [30], Lufa sponge [42], etc., but, is much smaller than many other lignocellulosic fibers such as *Calotropis gigantea* Bast [1], *Ferula communis* [2], *Furcraea foetida* [9], etc. Young's Modulus of the sample is estimated to be 1.05 ± 0.08 GPa, while the elongation at break is 18.94 ± 4.26%. The tensile properties of *Calamus tenuis* canes are shown in Fig. 5(b). Table 5, shows that there are significant disparities in tensile properties among the various natural fibers, which may be due to the variations in cellulose content and other components within the fibers, and differences in their internal structures [20]. On the other hand, the presumption of a circular cross-section of the samples as well as the defects present in the samples may be the reason for getting a relatively high value of standard error in the measurement of tensile properties of the *Calamus tenuis* canes [20,22]. The microfibrillar angle (MFA) is estimated from Eq. (7). and its value for *Calamus tenuis* cane fibers is found to be 34.22 ± 6.44°. The value of MFA for *Calamus tenuis* cane fibers is close to coir (30.45°) [55], Rachilla (35°-39°) [55], Rachis (28°-37°) [55], etc., and is smaller than Ramie (69°-83°) [56], *Rhectophyllum camerunense* (40.1 ± 0.5°) [56], etc. The natural fiber having higher MFA shows greater ductility properties as the microfibril angle of natural fiber varies directly with the strain applied. On the other hand, the fiber having lower MFA exhibits better mechanical properties as the microfibril angle inversely depends on its tensile strength and modulus of elasticity [28].

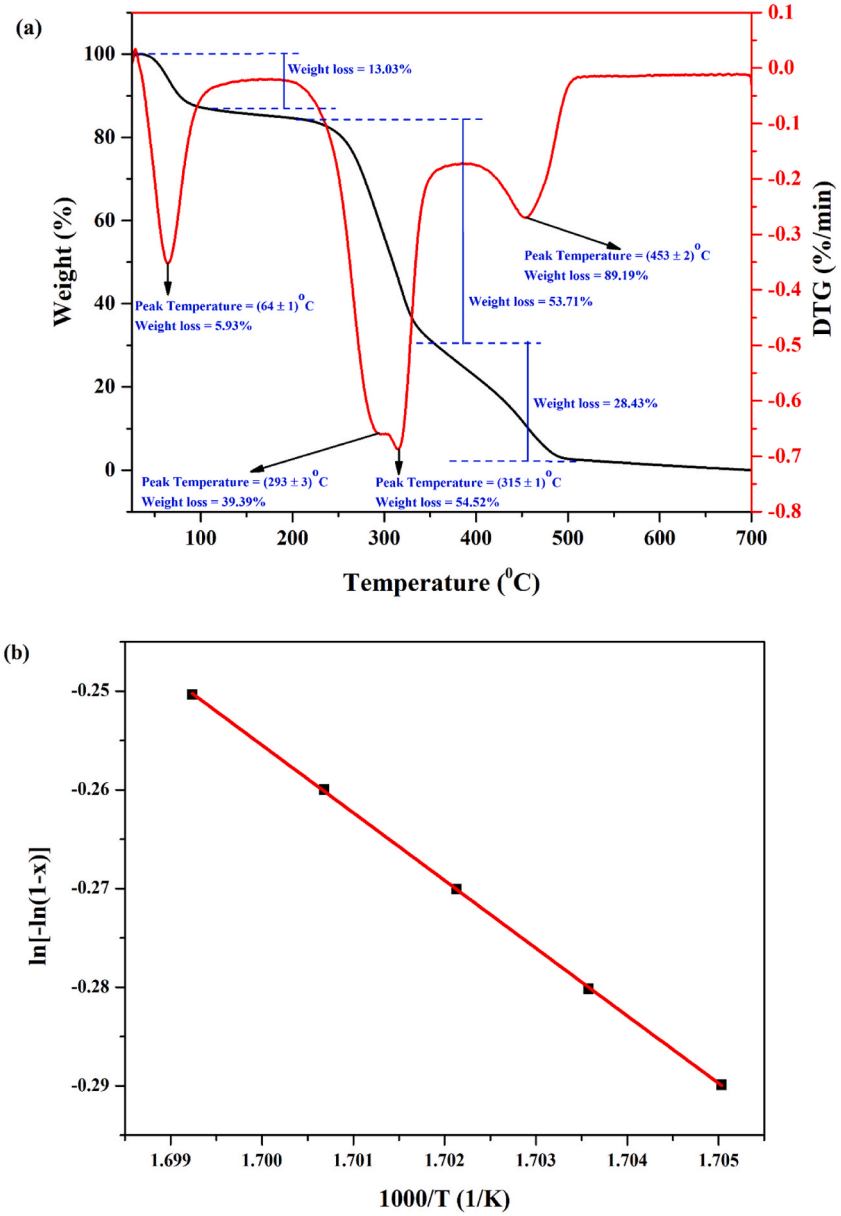

Fig. 4. (a) TGA and, DTG graph of *Calamus tenuis* cane fibers, (b) Plot for determination of kinetic activation energy.

Table 4
Comparison of Thermal properties of *Calamus tenuis* cane fibers with various natural fibers.

Name of Fibers	Thermal Stability (°C)	Hemicellulose Degradation Temperature (°C)	Maximum Degradation Temperature (°C)
Calamus tenuis	**210 ± 5**	**293 ± 3**	**315 ± 1**
Calotropis gigantea Bast [1]	200	–	360
Ferula communis [2]	>200		313.5
Chloris barbata [3]	210	254.5	324.6
Tridax procumbens [4]	195	250	330
Prosopis juliflora bark [8]	217	–	331.1
Furcraea foetida [9]	–	–	320.5
Calamus manan [20]	220	–	332.8
Cyrtostachys renda [21]	260	297.5	364.95
Arundo donax L. [22]	275	295	320
Cissus quadrangularis stem [27]	270	294.6	342.1
Coccinia grandis L. [28]	213.4	296.17	351.6
Corypha taliera fruit [30]	230	275.18	334.41
Juncus effusus L. [31,41]	220	281.4	332.6
Wikstroemia Spp. [33]	–	~250	315
Raffia textilis [34]	256	303	340
Furcraea foetida leaves [36]	204.04	–	356.75
Stipa tenacissima stem [37]	210	290	350
Agave americana L. [38]	–	–	366
Pennisetum purpureum stem [43]	–	306.6	264.7
Saharan Aloevera Cactus Leaves [45]	225	272	350
Areca Palm Leaf Stalk [48]	–	279	365
Ceiba aesculifolia Seed Pods [50]	220	315	352
Date Palm [51,52]	260	290	~310
Musa textilis [53]	–	298	335
Sugar Palm [54]	–	285.78	348.16

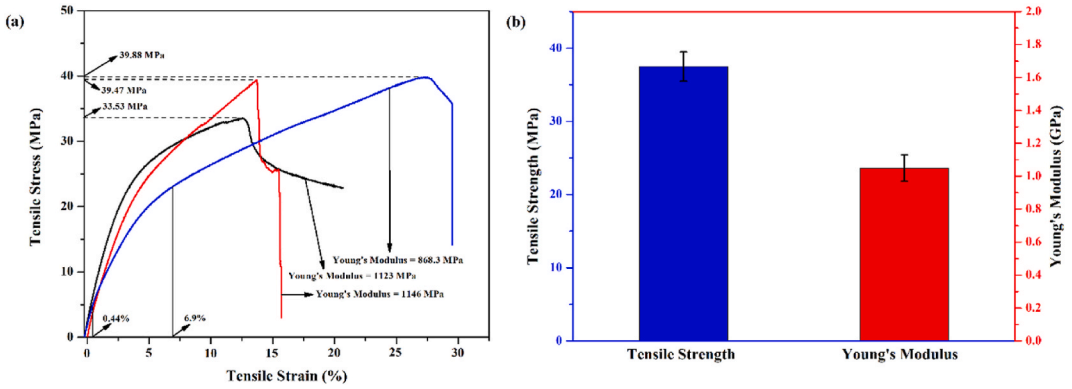

Fig. 5. **(a)** Tensile Stress – Tensile Strain curve of *Calamus tenuis* canes, **(b)** Tensile properties of *Calamus tenuis* canes.

3.6.2. Flexural test

Flexural Stress – Flexural Strain curve of *Calamus tenuis* canes is shown in Fig. 7(a) which exhibits three stages of deformation till failure. Initially, the graph is linear up to 0.005% of deformation which indicates the elastic behavior of *Calamus tenuis* canes. Thereafter the plastic deformation occurred non-linearly from the strain of about 0.005%–0.07%. Finally, the flexural strain increases linearly from 0.07% until it reaches the maximum value of flexural stress, where it underwent a sudden failure, which confirms the brittle nature of the samples [58]. Fig. 7(b) displays the flexural properties of *Calamus tenuis* canes. The maximum value of flexural stress is also called flexural strength or modulus of rupture (MOR) and it is calculated to be 60.52 ± 6.37 MPa, and flexural modulus is found to be 0.94 ± 0.04 GPa and it measures the degree of stiffness and the extent of deformation of the samples when a bending force is applied.

3.7. Scanning Electron Microscope (SEM) analysis

Fig. 8(a), (e), and 8(i) show the digital image of the cross-sectional view, longitudinal view (inner surface), and longitudinal view (outer surface) of *Calamus tenuis* canes. SEM images displayed in Fig. 8(b-d) and Fig. 8(f–h) reveal that *Calamus tenuis* canes are highly porous and composed of metaxylem (large-sized black empty space), protoxylem (black empty space), phloem (black empty space),

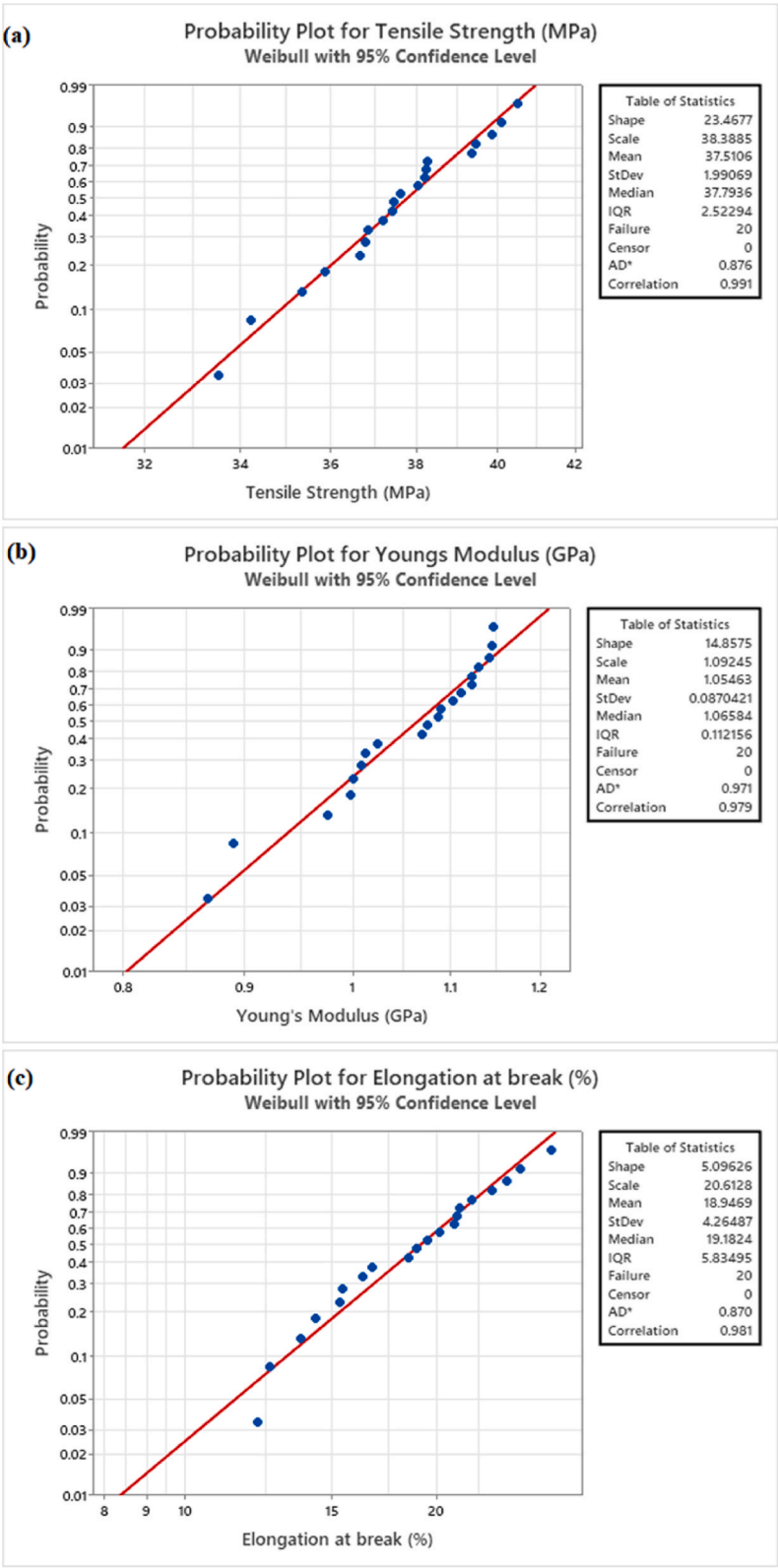

Fig. 6. Weibull distribution for (a) tensile strength, (b) Young's modulus, and (c) elongation at break of *Calamus tenuis* canes.

Table 5
Comparison of Tensile properties of *Calamus tenuis* canes with various natural fibers.

Name of fibers	Tensile Strength (MPa)	Young's Modulus (GPa)	Elongation at break (%)
Calamus tenuis	**37.5 ± 2**	**1.05 ± 0.08**	**18.94 ± 4.26**
Calotropis gigantea Bast [1]	629 ± 32.6	21.30 ± 2.40	3.50 ± 0.40
Ferula communis [2]	475.60 ± 15.70	52.70 ± 3.70	4.20 ± 0.20
Tridax procumbens [4]	25.75	0.94 ± 0.09	2.77 ± 0.27
Areca Palm Leaf Stalk [5]	334.66 ± 21.46	7.64 ± 1.13	4.38 ± 1.15
Prosopis juliflora bark [8]	558 ± 13.40	–	1.77 ± 0.04
Furcraea foetida [9]	605.25 ± 45.00	6.29 ± 1.90	10.56 ± 2.00
Calamus manan [20]	273.28 ± 52.88	7.8 ± 1.7	9.40 ± 3.67
Arundo donax L. [22]	248	9.4	3.24
Stipa tenacissima [24]	250	20	–
Acacia leucophloea [25]	317–1608	8.41–69.61	1.38–4.24
Calamus manan (Bulk) [26]	36.5	–	–
Coccinia grandis L. [28]	316.30 ± 36.63	10.17 ± 1.261	2.703 ± 0.273
Corn Husk [29]	160.49 ± 17.12	4.57 ± 0.54	21.08 ± 2.86
Corypha taliera fruit [30]	43.24	0.57221	–
Juncus effusus L. [31]	113 ± 36	4.38 ± 1.37	2.75 ± 0.68
Palm Tree Leaf Stalk [32]	74	9.50	–
Wikstroemia Spp. [33]	1187	–	2.48
Raffia textilis [34]	527 ± 84	26 ± 2	2.8 ± 0.7
Saccharum spontaneum [35]	337 ± 34	8.91 ± 0.18	–
Furcraea foetida leaves [36]	192.37 ± 21.45	7.45 ± 1.31	4.51 ± 0.73
Agave americana L. [38]	275 ± 15	8.60 ± 0.31	3.40 ± 0.20
Lufa Sponge [42]	33.54 ± 7.18	0.8202 ± 0.2195	6.67 ± 3.70
Pennisetum purpureum stem [43]	73 ± 6	5.68 ± 0.14	1.40 ± 0.23
Saharan Aloevera Cactus Leaves [45]	621.80	40.03	2.47
Date palm tree [52]	58–203	2–7.5	5–10
Cyrtostachys renda [57]	119	1.5	3.13

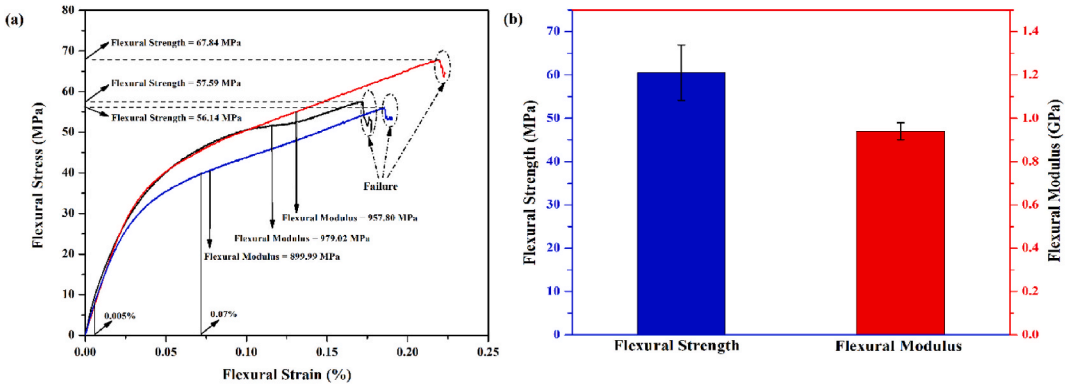

Fig. 7. (a) Flexural Stress – Flexural Strain curve of *Calamus tenuis* canes, (b) Flexural properties of *Calamus tenuis* canes.

dark grey coloured parenchyma cells and fibrous sheath, which supports the previous results [26,59,60]. SEM images displayed in Fig. 8(j-l), confirm that the surface of *Calamus tenuis* canes contains some unwanted impurities and wax-like substances. In addition, the surface has rough texture that improves the fiber - matrix interaction during the production of composites [27,61].

3.8. Atomic Force Microscope (AFM) analysis

Fig. 9(a) and (b) display the 2D and 3D AFM images of the surface of the *Calamus tenuis* cane fibers. The mean roughness (S_a) of raw *Calamus tenuis* cane fibers is found as 88.1 nm which is much higher than *Chloris barbata* (0.894 nm) [3], *Furcraea foetida* (18.005 nm) [9], *Acacia planifrons* (0.708 nm) [62], etc. but is lower than *Cyperus pangorei* (625 nm) [63]. The higher value of mean roughness (S_a) signifies the roughness of the surface. Some part of Fig. 9(a) and (b) exhibits smooth surfaces, which could be ascribed to the presence of non-cellulosic compounds such as lignin, pectin, hemicellulose, and a minimum amount of impurities on the fibers' surface. The calculated value of surface skewness (S_{sk}) is 0.3604, which quantifies the degree of asymmetry in the distribution of heights over the

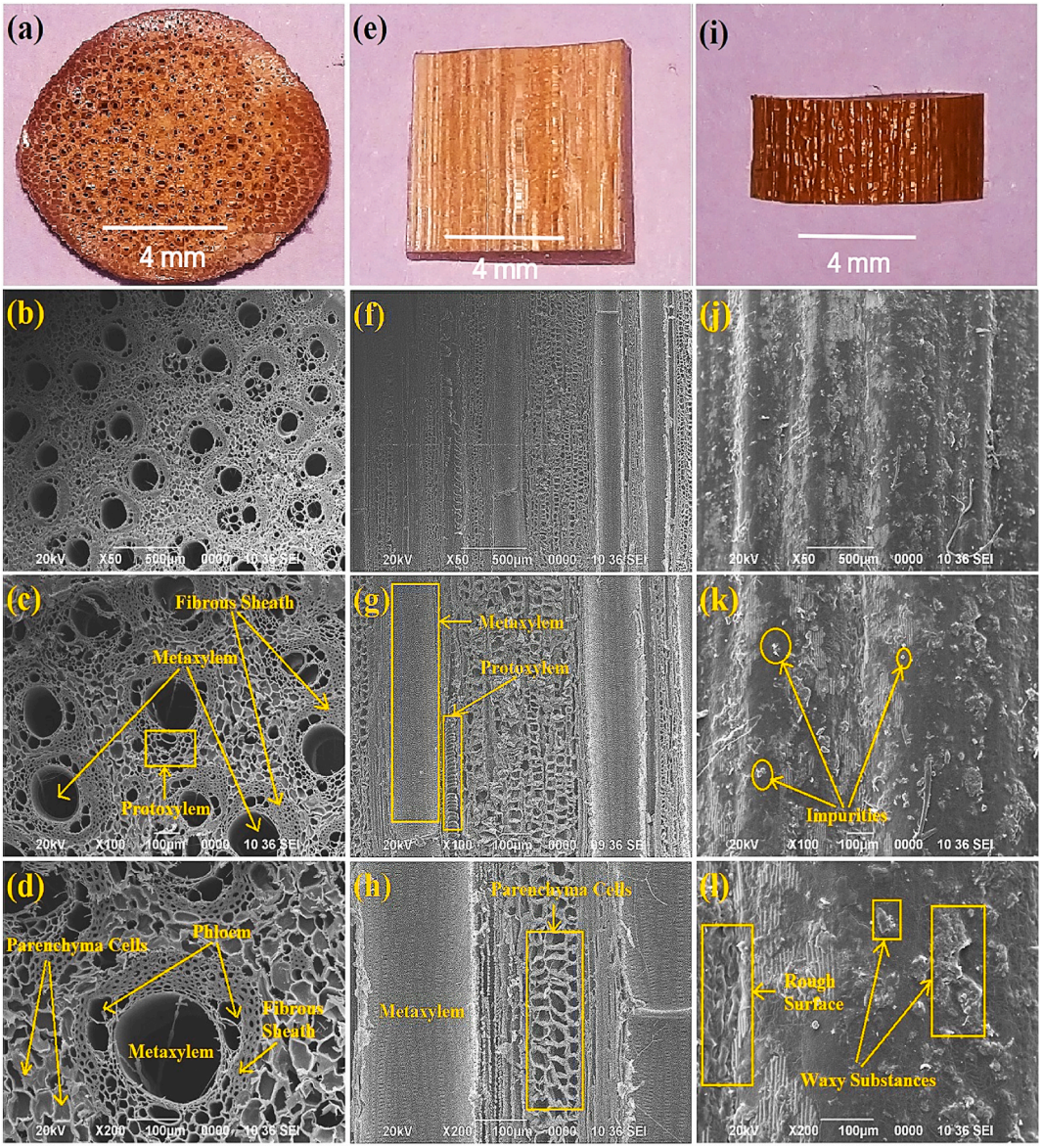

Fig. 8. (a) Digital image of the cross-sectional view of *Calamus tenuis* canes, (b)–(d): SEM micrograph of the cross-sectional view of *Calamus tenuis* canes at magnification 50×, 100×, and 200×. (e) Digital image of longitudinal view (inner surface) of *Calamus tenuis* canes, (f)–(h): SEM micrograph of longitudinal view (inner surface) of *Calamus tenuis* canes at magnification 50×, 100×, and 200×. (i) Digital image of longitudinal view (outer surface) of *Calamus tenuis* canes, (j)–(l): SEM micrograph of longitudinal view (outer surface) of *Calamus tenuis* canes at magnification 50×, 100×, and 200×.

sampled area [62]. The positive value of surface skewness (S_{sk}) indicates the nonporous nature of the surface [3]. The surface kurtosis (S_{ku}) value indicates the types of surfaces. $S_{ku} > 3$ indicates the spiky surface and if $S_{ku} < 3$, meaning the surface is rough [9]. In this work, the value of S_{ku} is 0.7985, which implies the surface is rough. The above observation is also confirmed by the higher values of S_t (363.5 nm), S_z (224.9 nm), and S_q (115.7 nm) respectively.

4. Conclusion

This work investigates the physio-chemical, structural, thermal, mechanical properties, and morphological properties of the *Calamus tenuis* cane fibers. Chemical analysis confirms that the *Calamus tenuis* cane fibers contain 37.43 ± 1.40% cellulose, 31.06 ± 1.03% hemicellulose, 28.42 ± 0.81% lignin, 10.57 ± 1.53% moisture, and very less amount of pectin and ash. FTIR analysis also confirms the presence of these constituents in the sample. The low value of the density (526 ± 16 kg m^{-3}) of *Calamus tenuis* cane fibers reveals that these natural fibers are suitable for lightweight bio-composite applications. The fibers of *Calamus tenuis* show a

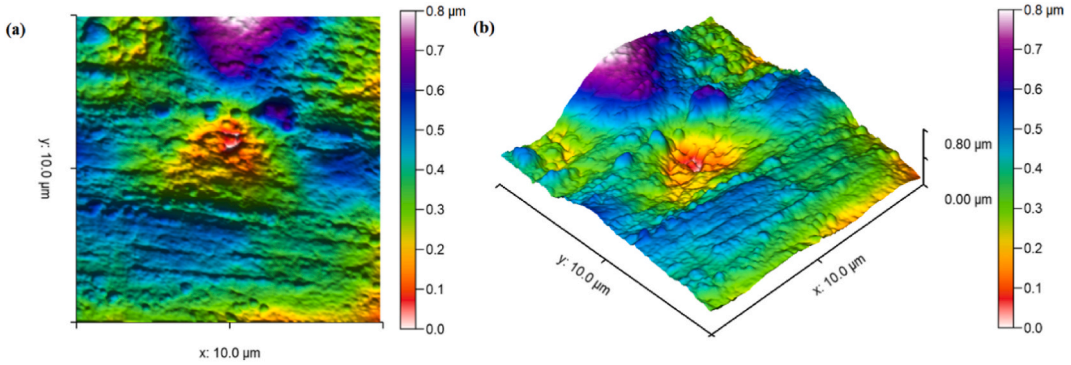

Fig. 9. AFM images of (a) *Calamus tenuis* fibers in 2D, and (b) *Calamus tenuis* fibers in 3D.

crystallinity index of 37.38 ± 0.27% and a crystallite size of 0.87 ± 0.03 nm. The *Calamus tenuis* cane fibers exhibit thermal stability up to 210 ± 5 °C with activation energy 57.01 kJ/mol, which makes these fibers suitable to use as reinforcement elements for bio-composites that can operate up to 315 ± 1 °C. The tensile strength, young's modulus, and elongation at break of *Calamus tenuis* canes are estimated to be 37.5 ± 2 MPa, 1.05 ± 0.08 GPa, and 18.94 ± 4.26% respectively. The flexural strength and Flexural modulus of the canes are estimated as 60.52 ± 6.37 MPa, and, 0.94 ± 0.04 GPa respectively. SEM micrographs reveal the porous structure and rough outer surface of *Calamus tenuis* canes, which is also confirmed by AFM images and various roughness parameters evaluated from AFM analysis, which will provide better fiber-matrix adhesion during the fabrication of composites. These significant properties of the *Calamus tenuis* cane fibers suggest that these fibers could be considered as a potential reinforcement for polymer composites.

Author contribution statement

Arup Kar; Dip Saikia: Conceived and designed the experiments; Performed the experiments; Analyzed and interpreted the data; Contributed reagents, materials, analysis tools or data; Wrote the paper.

Data availability statement

The authors do not have permission to share data.

Declaration of competing interest

The authors declare that they have no known competing financial interests or personal relationships that could have appeared to influence the work reported in this paper.

Acknowledgment

We extend our sincere gratitude and appreciation to, CSIR-NEIST Jorhat, Assam (India) for granting us access to their chemical analysis facility. Additionally, we express our thanks to the Earth Science Department, IIT Kanpur, Uttar Pradesh (India) for providing us with the Gas Pycnometer for density analysis. We are also grateful to SAIC, Tezpur University, Tezpur, Assam (India) for the FTIR and SEM facilities and to SAIC, IASST Guwahati, Assam (India) for the AFM facilities. Furthermore, we acknowledge SAIF, Gauhati University, Guwahati, Assam (India) for providing us with the PXRD and TGA facilities. Lastly, we would like to thank Mr. Sanjib Sarma, IIT Guwahati, Assam (India), for allowing us to use their laboratory facility for tensile and flexural tests.

References

[1] R. Ramasamy, K. Obi Reddy, A. Varada Rajulu, Extraction and characterization of *Calotropis gigantea* Bast fibers as novel reinforcement for composites materials, J. Nat. Fibers 15 (2018) 527–538, https://doi.org/10.1080/15440478.2017.1349019.
[2] Y. Seki, M. Sarikanat, K. Sever, C. Durmuşkahya, Extraction and properties of *Ferula communis* (chakshir) fibers as novel reinforcement for composites materials, Compos. B Eng. 44 (2013) 517–523, https://doi.org/10.1016/j.compositesb.2012.03.013.
[3] P. Balasundar, P. Narayanasamy, P. Senthamaraikannan, S. Senthil, R. Prithivirajan, T. Ramkumar, Extraction and characterization of new natural cellulosic *Chloris barbata* fiber, J. Nat. Fibers 15 (2018) 436–444, https://doi.org/10.1080/15440478.2017.1349015.
[4] R. Vijay, D. Lenin Singaravelu, A. Vinod, M.R. Sanjay, S. Siengchin, M. Jawaid, et al., Characterization of raw and alkali treated new natural cellulosic fibers from *Tridax procumbens*, Int. J. Biol. Macromol. 125 (2019) 99–108, https://doi.org/10.1016/j.ijbiomac.2018.12.056.
[5] N. Shanmugasundaram, I. Rajendran, T. Ramkumar, Characterization of untreated and alkali treated new cellulosic fiber from an Areca palm leaf stalk as potential reinforcement in polymer composites, Carbohydr. Polym. 195 (2018) 566–575, https://doi.org/10.1016/j.carbpol.2018.04.127.
[6] A.Q. Dayo, A. Zegaoui, A.A. Nizamani, S. Kiran, J. Wang, M. Derradji, et al., The influence of different chemical treatments on the hemp fiber/polybenzoxazine based green composites: mechanical, thermal and water absorption properties, Mater. Chem. Phys. 217 (2018) 270–277, https://doi.org/10.1016/J.MATCHEMPHYS.2018.06.040.

[7] B.Ly E. hadji, J. Bras, P. Sadocco, M.N. Belgacem, A. Dufresne, W. Thielemans, Surface functionalization of cellulose by grafting oligoether chains, Mater. Chem. Phys. 120 (2010) 438–445, https://doi.org/10.1016/J.MATCHEMPHYS.2009.11.032.

[8] S.S. Saravanakumar, A. Kumaravel, T. Nagarajan, P. Sudhakar, R. Baskaran, Characterization of a novel natural cellulosic fiber from *Prosopis juliflora* bark, Carbohydr. Polym. 92 (2013) 1928, https://doi.org/10.1016/j.carbpol.2012.11.064. –33.

[9] P. Manimaran, P. Senthamaraikannan, M.R. Sanjay, M.K. Marichelvam, M. Jawaid, Study on characterization of *Furcraea foetida* new natural fiber as composite reinforcement for lightweight applications, Carbohydr. Polym. 181 (2018) 650–658, https://doi.org/10.1016/j.carbpol.2017.11.099.

[10] K.M. Muthukrishnan, G. Selvakumar, P. Narayanasamy, P. Ravindran, Characterization of raw and alkali treated cellulosic filler isolated from *Putranjiva roxburghii* W. Seed Shell roadside vegetative residues, J. Nat. Fibers 19 (2022) 14287–14298, https://doi.org/10.1080/15440478.2022.2061670.

[11] S.A.S. Biswas, et al., Indian rattans (canes): diversity, distribution and propagation, Indian For. 121 (1995) 620–633.

[12] D. Saikia, Studies on Thermo-Physical Properties of Some Textile Fibres (Plant), Available in North East India, Ph.D. Thesis, Gauhati University, 2003.

[13] E.S. Jang, C.W. Kang, Changes in gas permeability and pore structure of wood under heat treating temperature conditions, J. Wood Sci. 65 (2019), https://doi.org/10.1186/s10086-019-1815-3.

[14] S.H. Park, J.H. Jang, N.J. Wistara, W. Hidayat, M. Lee, F. Febrianto, Anatomical and physical properties of Indonesian bamboos carbonized at different temperatures, J. Korean Wood Sci. Technol. 46 (2018) 656–669, https://doi.org/10.5658/WOOD.2018.46.6.656.

[15] A.B. Das, Separation, Purification and Application of Bioactive Compounds from Pigmented Rice Bran, Ph.D. Thesis, Indian Institute of Technology, Guwahati, 2020.

[16] L. Dampanaboina, N. Yuan, V. Mendu, Estimation of crystalline cellulose content of plant biomass using the Undegraff method, J. Vis. Exp. (2021), https://doi.org/10.3791/62031.

[17] C.V. Agu, O.U. Njoku, F.C. Chilaka, D. Agbiogwu, K.V. Iloabuchi, B. Ukazu, Physicochemical properties of lignocellulosic biofibres from South Eastern Nigeria: their suitability for biocomposite technology, Afr. J. Biotechnol. 13 (2014) 2050, https://doi.org/10.5897/AJB2013.13443. –7.

[18] L. Segal, J.J. Creely, A.E. Martin, C.M. Conrad, An empirical method for estimating the degree of crystallinity of native cellulose using the X-ray diffractometer, Textil. Res. J. 29 (1959) 786–794, https://doi.org/10.1177/004051755902901003.

[19] M.A. Farrukh, K.M. Butt, K.K. Chong, W.S. Chang, Photoluminescence emission behavior on the reduced band gap of Fe doping in CeO_2-SiO_2 nanocomposite and photophysical properties, J. Saudi Chem. Soc. 23 (2019) 561–575, https://doi.org/10.1016/j.jscs.2018.10.002.

[20] L. Ding, X. Han, L. Cao, Y. Chen, Z. Ling, J. Han, et al., Characterization of natural fiber from manau rattan (*Calamus manan*) as a potential reinforcement for polymer-based composites, J. Bioresour. Bioprod. (2021), https://doi.org/10.1016/J.JOBAB.2021.11.002.

[21] T.M. Loganathan, M.T.H. Sultan, Q. Ahsan, M. Jawaid, J. Naveen, M.A.U. Shah AU, et al., Characterization of alkali treated new cellulosic fibre from *Cyrtostachys renda*, J. Mater. Res. Technol. 9 (2020) 3537–3546, https://doi.org/10.1016/j.jmrt.2020.01.091.

[22] V. Fiore, T. Scalici, A. Valenza, Characterization of a new natural fiber from *Arundo donax* L. as potential reinforcement of polymer composites, Carbohydr. Polym. 106 (2014) 77–83, https://doi.org/10.1016/j.carbpol.2014.02.016.

[23] A.K. Bledzki, O. Faruk, V.E. Sperber, Cars from bio-fibres, Macromol. Mater. Eng. 291 (2006) 449–457, https://doi.org/10.1002/mame.200600113.

[24] M.C. Paiva, I. Ammar, A.R. Campos, R.B. Cheikh, A.M. Cunha, Alfa fibres: mechanical, morphological and interfacial characterization, Compos. Sci. Technol. 67 (2007) 1132–1138, https://doi.org/10.1016/j.compscitech.2006.05.019.

[25] V.P. Arthanarieswaran, A. Kumaravel, S.S. Saravanakumar, Physico-chemical properties of alkali-treated *Acacia leucophloea* fibers, Int. J. Polym. Anal. Char. 20 (2015) 704–713, https://doi.org/10.1080/1023666X.2015.1081133.

[26] X. Han, L. Ding, Z. Tian, W. Wu, S. Jiang, Extraction and characterization of novel ultrastrong and tough natural cellulosic fiber bundles from manau rattan (*Calamus manan*), Ind. Crop. Prod. 173 (2021), https://doi.org/10.1016/j.indcrop.2021.114103.

[27] S. Indran, R.E. Raj, Characterization of new natural cellulosic fiber from *Cissus quadrangularis* stem, Carbohydr. Polym. 117 (2015) 392–399, https://doi.org/10.1016/j.carbpol.2014.09.072.

[28] P. Senthamaraikannan, M. Kathiresan, Characterization of raw and alkali treated new natural cellulosic fiber from *Coccinia grandis* L, Carbohydr. Polym. 186 (2018) 332–343, https://doi.org/10.1016/j.carbpol.2018.01.072.

[29] S.N. Herlina, I.N.G. Wardana, Y.S. Irawan, E. Siswanto, Characterization of the chemical, physical, and mechanical properties of NaOH-treated natural cellulosic fibers from corn husks, J. Nat. Fibers 15 (2018) 545–558, https://doi.org/10.1080/15440478.2017.1349707.

[30] T.A. Tamanna, S.A. Belal, M.A.H. Shibly, A.N. Khan, Characterization of a new natural fiber extracted from *Corypha taliera* fruit, Sci. Rep. 11 (2021), https://doi.org/10.1038/s41598-021-87128-8.

[31] M. Maache, A. Bezazi, S. Amroune, F. Scarpa, A. Dufresne, Characterization of a novel natural cellulosic fiber from *Juncus effusus* L, Carbohydr. Polym. 171 (2017) 163–172, https://doi.org/10.1016/j.carbpol.2017.04.096.

[32] A.K. Rout, J. Kar, D.K. Jesthi, A.K. Sutar, Effect of surface treatment on the physical, chemical, and mechanical properties of palm tree leaf stalk fibers, Bioresources 11 (2016) 4432–4445, https://doi.org/10.15376/biores.11.2.4432-4445.

[33] M. Pouriman, A.R. Caparanga, M. Ebrahimi, A. Dahresobh, Characterization of untreated and alkaline-treated salago fibers (*genus Wikstroemia spp.*), J. Nat. Fibers 15 (2018) 296–307, https://doi.org/10.1080/15440478.2017.1329105.

[34] R.G. Elenga, P. Djemia, D. Tingaud, T. Chauveau, J.G. Maniongui, G. Dirras, Effects of alkali treatment on the microstructure, composition, and properties of the *Raffia textilis* fiber, Bioresources 8 (2013) 2934–2949, https://doi.org/10.15376/biores.8.2.2934-2949.

[35] G.L. Devnani, S. Sinha, Extraction, characterization and thermal degradation kinetics with activation energy of untreated and alkali treated *Saccharum spontaneum* (Kans grass) fiber, Compos. B Eng. 166 (2019) 436–445, https://doi.org/10.1016/j.compositesb.2019.02.042.

[36] S.M. Shahril, M.J.M. Ridzuan, M.S.A. Majid, A.M.N. Bariah, M.T.A. Rahman, P. Narayanasamy, Alkali treatment influence on cellulosic fiber from *Furcraea foetida* leaves as potential reinforcement of polymeric composites, J. Mater. Res. Technol. 19 (2022) 2567–2583, https://doi.org/10.1016/j.jmrt.2022.06.002.

[37] K.E. Borchani, C. Carrot, M. Jaziri, Untreated and alkali treated fibers from Alfa stem: effect of alkali treatment on structural, morphological and thermal features, Cellulose 22 (2015) 1577–1589, https://doi.org/10.1007/s10570-015-0583-5.

[38] K.O. Reddy, K.R.N. Reddy, J. Zhang, J. Zhang, A. Varada Rajulu, Effect of alkali treatment on the properties of century fiber, J. Nat. Fibers 10 (2013) 282–296, https://doi.org/10.1080/15440478.2013.800812.

[39] S.W. Saragih, R. Lubis, B. Wirjosentono, Eddyanto, characteristic of abaca (*Musa textilis*) fiber from aceh Timur as bioplastic, AIP Conf. Proc. 2049 (2018), https://doi.org/10.1063/1.5082463.

[40] A.B. Mabrouk, H. Kaddami, S. Boufi, F. Erchiqui, A. Dufresne, Cellulosic nanoparticles from alfa fibers (*Stipa tenacissima*): extraction procedures and reinforcement potential in polymer nanocomposites, Cellulose 19 (2012) 843–853, https://doi.org/10.1007/s10570-012-9662-z.

[41] L. Xia, C. Zhang, A. Wang, Y. Wang, W. Xu, Morphologies and properties of *Juncus effusus* fiber after alkali treatment, Cellulose 27 (2020) 1909, https://doi.org/10.1007/s10570-019-02933-9. –20.

[42] Y. Chen, N. Su, K. Zhang, S. Zhu, Z. Zhu, W. Qin, et al., Effect of fiber surface treatment on structure, moisture absorption and mechanical properties of luffa sponge fiber bundles, Ind. Crop. Prod. 123 (2018) 341–352, https://doi.org/10.1016/j.indcrop.2018.06.079.

[43] M.J.M. Ridzuan, M.S. Abdul Majid, M. Afendi, S.N. Aqmariah Kanafiah, J.M. Zahri, A.G. Gibson, Characterisation of natural cellulosic fibre from *Pennisetum purpureum* stem as potential reinforcement of polymer composites, Mater. Des. 89 (2016) 839–847, https://doi.org/10.1016/j.matdes.2015.10.052.

[44] K.O. Reddy, C.U. Maheswari, M. Shukla, A.V. Rajulu, Chemical composition and structural characterization of Napier grass fibers, Mater. Lett. 67 (2012) 35–38, https://doi.org/10.1016/j.matlet.2011.09.027.

[45] A.N. Balaji, K.J. Nagarajan, Characterization of alkali treated and untreated new cellulosic fiber from Saharan aloe vera cactus leaves, Carbohydr. Polym. 174 (2017) 200–208, https://doi.org/10.1016/j.carbpol.2017.06.065.

[46] M. Cai, H. Takagi, A.N. Nakagaito, Y. Li, G.I.N. Waterhouse, Effect of alkali treatment on interfacial bonding in abaca fiber-reinforced composites, Compos. Part A. Appl. Sci. Manuf. 90 (2016) 589–597, https://doi.org/10.1016/j.compositesa.2016.08.025.

[47] D. Saikia, Investigations on structural characteristics, thermal stability, and hygroscopicity of sisal fibers at elevated temperatures, Int. J. Thermophys. 29 (2008) 2215–2225, https://doi.org/10.1007/s10765-008-0539-1.

[48] R.P.G. Ranganagowda, S.S. Kamath, B. Bennehalli, Extraction and characterization of cellulose from natural Areca fiber, Mater. Sci. Res. Int. 16 (2019) 86–93, https://doi.org/10.13005/msri/160112.
[49] N. di Fidio, A.M.R. Galletti, S. Fulignati, D. Licursi, F. Liuzzi, I. de Bari, et al., Multi-step exploitation of raw *Arundo donax* L. For the selective synthesis of second-generation sugars by chemical and biological route, Catalysts 10 (2020), https://doi.org/10.3390/catal10010079.
[50] U. Carranza-Nuñez, S.R. Vasquez-Garcia, N. Flores-Ramirez, H.A. Abdel-Gawwad, J.L. Rico, A. Arizbe Santiago, J. Vargas, J. Cruz-de-León, Physicochemical characterization of natural fibers obtained from seed pods of *Ceiba aesculifolia*, Bioresources 16 (2021) 4200–4211.
[51] A. Oushabi, S. Sair, F. Oudrhiri Hassani, Y. Abboud, O. Tanane, A. el Bouari, The effect of alkali treatment on mechanical, morphological and thermal properties of date palm fibers (DPFs): study of the interface of DPF–Polyurethane composite, S. Afr. J. Chem. Eng. 23 (2017) 116–123, https://doi.org/10.1016/j.sajce.2017.04.005.
[52] A. Alawar, A.M. Hamed, K. Al-Kaabi, Characterization of treated date palm tree fiber as composite reinforcement, Compos. B Eng. 40 (2009) 601–606, https://doi.org/10.1016/j.compositesb.2009.04.018.
[53] R.A.J. Malenab, J.P.S. Ngo, M.A.B. Promentilla, Chemical treatment of waste abaca for natural fiber-Reinforced geopolymer composite, Materials 10 (2017), https://doi.org/10.3390/ma10060579.
[54] B. Rashid, Z. Leman, M. Jawaid, M.J. Ghazali, M.R. Ishak, Physicochemical and thermal properties of lignocellulosic fiber from sugar palm fibers: effect of treatment, Cellulose 23 (2016) 2905–2916, https://doi.org/10.1007/s10570-016-1005-z.
[55] T. Sathishkumar, P. Navaneethakrishnan, S. Shankar, R. Rajasekar, N. Rajini, Characterization of natural fiber and composites – a review, J. Reinforc. Plast. Compos. 32 (2013) 1457–1476, https://doi.org/10.1177/0731684413495322.
[56] A. Béakou, R. Ntenga, J. Lepetit, J.A. Atéba, L.O. Ayina, Physico-chemical and microstructural characterization of "*Rhectophyllum camerunense*" plant fiber, Compos. Part A. Appl. Sci. Manuf. 39 (2008) 67–74, https://doi.org/10.1016/j.compositesa.2007.09.002.
[57] T.M. Loganathan, M.T.H. Sultan, M. Jawaid, Q. Ahsan, J. Naveen, A.U.M. Shah, et al., Physical, mechanical, and morphological properties of hybrid *Cyrtostachys renda*/kenaf fiber reinforced with multi-walled carbon nanotubes (MWCNT)-phenolic composites, Polymers 13 (2021), https://doi.org/10.3390/polym13193448.
[58] A. Gopinath, M.S. Kumar, A. Elayaperumal, Experimental investigations on mechanical properties of jute fiber reinforced composites with polyester and epoxy resin matrices, Procedia Eng. 97 (2014) 2052–2063, https://doi.org/10.1016/j.proeng.2014.12.448.
[59] J. Li, R. Ma, Y. Lu, Z. Wu, M. Su, K. Jin, et al., A gravity-driven high-flux catalytic filter prepared using a naturally three-dimensional porous rattan biotemplate decorated with Ag nanoparticles, Green Chem. 22 (2020) 6846–6854, https://doi.org/10.1039/D0GC01709D.
[60] P.B. Tomlinson, J.B. Fisher, R.E. Spangler, R.A. Richer, Stem vascular architecture in the rattan palm *Calamus* (Arecaceae-Calamoideae-Calaminae), Am. J. Bot. 88 (2001) 797–809.
[61] L. Yan, N. Chouw, X. Yuan, Improving the mechanical properties of natural fibre fabric reinforced epoxy composites by alkali treatment, J. Reinforc. Plast. Compos. 31 (2012) 425–437, https://doi.org/10.1177/0731684412439494.
[62] P. Senthamaraikannan, S.S. Saravanakumar, V.P. Arthanarieswaran, P. Sugumaran, Physico-chemical properties of new cellulosic fibers from the bark of *Acacia planifrons*, Int. J. Polym. Anal. Char. 21 (2016) 207–213, https://doi.org/10.1080/1023666X.2016.1133138.
[63] K. Mayandi, N. Rajini, P. Pitchipoo, J.T.W. Jappes, A.V. Rajulu, Extraction and characterization of new natural lignocellulosic fiber *Cyperus pangorei*, Int. J. Polym. Anal. Char. 21 (2016) 175–183, https://doi.org/10.1080/1023666X.2016.1132064.